Published in final edited form as:
Mol Cell. 2009 January 30; 33(2): 171–180. doi:10.1016/j.molcel.2009.01.001.

Actin Homologue MreB Affects Chromosome Segregation by Regulating Topoisomerase IV in *Escherichia coli*

Ram Madabhushi[1] and **Kenneth J. Marians**[1,2,3]

[1] Programs in Molecular Biology, Weill Graduate School of Cornell University, New York, NY 10075, USA

[2] Memorial Sloan-Kettering Cancer Center, New York, NY 10075, USA

SUMMARY

In *Escherichia coli*, topoisomerase IV, a type II topoisomerase, mediates the resolution of topological linkages between replicated daughter chromosomes and is essential for chromosome segregation. Topo IV activity is restricted to only a short interval late in the cell cycle. However, the mechanism that confers this temporal regulation is unknown. Here we report that the bacterial actin homologue, MreB, participates in the temporal oscillation of Topo IV activity. We show that *mreB* mutant strains are deficient in Topo IV activity. In addition, we demonstrate that depending upon whether it is in a monomeric or polymerized state, MreB affects Topo IV activity differentially. In addition, MreB physically interacts with the ParC subunit of Topo IV. Together these results may explain how dynamics of the bacterial cytoskeleton are coordinated with the timing of chromosome segregation.

Keywords

topoisomerase IV; MreB; decatenation; kinetoplast; cytoskeleton

INTRODUCTION

Accurate transmission of a cell's genetic material relies not only on the mechanics of chromosome segregation, but also on mechanisms that coordinate partitioning of chromosomes with other events of the cell cycle such as DNA replication, cytokinesis, and cell division. Although much is known about eukaryotic chromosome segregation, the mechanisms that orchestrate the timing of bacterial chromosome segregation have remained largely obscure. *Escherichia coli* has a single circular chromosome. Replication of this circular chromosome results in the formation of topologically linked daughter molecules. To complete chromosome segregation, these daughter chromosomes must be unlinked. This disentanglement is catalyzed by topoisomerase IV (Topo IV), a type II enzyme (Adams et al., 1992; Peng and Marians, 1993). Topo IV activity is therefore indispensable for completing chromosome segregation in *E. coli* (Kato et al., 1990; Kato et al., 1988).

Topo IV is a tetramer of two homodimers encoded by *parC* and *parE* (Kato et al., 1990; Peng and Marians, 1993). Two studies have suggested that Topo IV activity is both spatially and

3To whom correspondence should be sent, Tel. 212-639-5890, Fax. 212-717-3627, Email: kmarians@sloankettering.edu.

temporally regulated during the bacterial cell cycle (Espeli et al., 2003a; Wang and Shapiro, 2004). Fluorescence microscopy revealed that ParC and ParE maintained different localization patterns for most of the cell cycle. In *E. coli*, ParC co-localized with the replication machinery, whereas ParE localized to DNA-free spaces in the cell (Espeli et al., 2003a). In *Caulobacter crescentus*, ParC formed a sharp focus at mid-cell in a cell cycle dependent manner, whereas ParE was found dispersed throughout the cell (Wang and Shapiro, 2004). In addition, quinolone-induced, Topo IV-mediated cell killing was measured as a function of the cell cycle (Espeli et al., 2003a). Quinolones trap both DNA gyrase and Topo IV in a topo-quinolone-DNA ternary complex. A collision between this complex and the replication fork produces double-strand breaks (DSBs) that are capped by covalently bound proteins. The inability to repair such breaks presumably accounts for the cytotoxicity of these drugs (Espeli and Marians, 2004). In a synchronous population of *E. coli* where gyrase was mutated to quinolone-resistance, quinolone-induced cell killing occurred only late in the cell cycle (Espeli et al., 2003a). Although these results suggest that the temporal regulation of Topo IV activity is likely achieved by different spatial localizations of ParC and ParE for most of the cell cycle, the precise mechanism that confers the observed oscillation in Topo IV activity has remained elusive.

A renewed interest in bacterial chromosome segregation has been spurred by the identification of proteins in bacteria with significant homology to eukaryotic cytoskeletal elements (reviewed in Carballido-Lopez, 2006; and Shih and Rothfield, 2006). Of particular interest has been the bacterial actin orthologue, MreB, which forms helical filaments beneath the cell membrane and performs important functions in the maintenance of cell shape, lateral wall synthesis, determination of cell polarity, chromosome segregation, and cell division (Carballido-Lopez, 2006). MreB forms a complex with MreC, MreD, Pbp2, RodA, and MurG (Kruse et al., 2005; Mohammadi et al., 2007), further underscoring its role in cell wall synthesis. The MreB helix is probably anchored to the cell membrane via its interaction with MreC and MreD.

The discovery of cytoskeletal elements raised the possibility that bacteria utilize force-generating mechanisms analogous to the microtubule spindle to segregate their chromosomes. In support of this idea, analysis of *mreB* mutants in *E. coli* has suggested that a dysfunctional MreB causes defects in chromosome segregation (Kruse et al., 2003). In *ΔmreB* mutants, chromosomes seemed to segregate in pairs and overexpression of dominant-negative alleles of *mreB* in wild-type cells blocked chromosome segregation and cell division (Kruse et al., 2003). Furthermore, *oriC* and *TerC* were mis-localized in *mreB* mutants and either depletion or inhibition of MreB blocked bipolar migration of origins (Gitai et al., 2005; Kruse et al., 2006; Kruse et al., 2003; Soufo and Graumann, 2003). In contrast, it was shown recently that unlike the defects with movements of origin regions, topographic separation of chromosomes itself remains unaffected by MreB inhibition (Gitai et al., 2005; Kruse et al., 2006). Similarly, another study suggested that inhibition of MreB affects neither bipolar segregation of origin regions nor the topographic separation of chromosomes in *E. coli* (Karczmarek et al., 2007). Together, these results suggest that if MreB functions in chromosome segregation, it does not do so by working as a force-generating apparatus like the bipolar microtubule spindle that segregates eukaryotic chromosomes.

We report here that the defects in chromosome segregation in *mreB* mutant strains can be attributed to a deficiency in Topo IV activity. In addition, MreB interacts functionally and physically with Topo IV. This functional interaction is dependent on the oligomeric state of MreB – monomeric MreB inhibits Topo IV activity, whereas polymerized MreB stimulates it. Implications of this regulation on bacterial chromosome segregation are considered.

RESULTS

Nucleoids from *mreB* Mutant Strains Are Larger than Nucleoids from Wild-type Cells

The phenotype obtained by overexpressing dominant-negative alleles of *mreB* (Kruse et al., 2003) closely resembles the partition-defective (*par*) phenotype exhibited by Topo IV mutants (Kato et al., 1990; Kato et al., 1988). This observation raised the possibility that *mreB* mutants were deficient in Topo IV activity. However, a *par* phenotype could result from other reasons as well, such as a failure to complete DNA replication, defects in DNA condensation/supercoiling, or activation of a cell cycle checkpoint (Espeli et al., 2003a; Sawitzke and Austin, 2000). To distinguish between these possibilities, nucleoids were isolated by sedimentation under stabilizing conditions that prevent their decompaction (Zimmerman and Murphy, 2001), visualized by fluorescence microscopy, and their areas measured. Among the population of purified nucleoids, a subset of dumbbell-shaped nucleoids was observed (Figure 1B). These dumbbell-shaped nucleoids were intriguing because they resembled nucleoids in the cell that were in the terminal stages of chromosome segregation and had to be unlinked. To test if this was indeed the case, C600 cells carrying a temperature-sensitive allele of *parC* (C600*parC1215*) were shifted to a semi-restrictive temperature of 37 °C for 40 min. Nucleoids were then purified from these cells and the incidence of dumbbell-shaped nucleoids was assessed (Figure 1C). In contrast to wild-type C600 cells, blocking chromosome segregation by inactivating Topo IV in C600*parC1215* significantly increased the predominance of dumbbell-shaped nucleoids.

To test whether these dumbbell-shaped nucleoids could be resolved by Topo IV, nucleoids from C600 and C600*parC1215* cells were treated with Topo IV *in vitro* and the incidence of dumbbell-shaped nucleoids was quantified (Figure 1C). Whereas Topo IV treatment did not reduce the incidence of dumbbells in nucleoid preparations from wild-type C600 cells, it reduced the incidence of dumbbells in nucleoid preparations from C600*parC1215* cells to wild-type levels. Together, two conclusions can be drawn from these observations: (1) Dumbbell-shaped nucleoids represent intermediates of chromosome segregation and (2), only a subset of these dumbbell-shaped nucleoids can be resolved by treatment with Topo IV, presumably those that correspond to nucleoids that need to be unlinked following replication. These observations recapitulate previous observations on dumbbell-shaped nucleoids (Steck and Drlica, 1984).

Based on the observations above, nucleoids were prepared from PA340 (wild type) and PA340-678 (*Δmre;* deleted for *mreB*, *mreC*, and *mreD*). The size distribution of nucleoids from the *Δmre* strain differed significantly than that of the wild type (Figure 2A). Whereas 80% of the nucleoids from the wild type had an area less than 2 μm^2, nucleoids from the *Δmre* mutants were larger and populated higher size classes. Nucleoids from the *Δmre* strain (mean area 3 μm^2) were twice as large as nucleoids purified from wt (mean area 1.6 μm^2). To test whether the observed difference was dependent on MreB, PA340-678 cells were transformed with a plasmid carrying *mreB* under the control of an *araC* promoter. Nucleoids were isolated from these cells grown in the presence of arabinose and characterized as before (Figure 2A). Overexpression of *mreB* in *Δmre* mutants restored the size distribution of nucleoids (mean area 1.4 μm^2) to a wild-type pattern.

The prevalence of dumbbell-shaped nucleoids in nucleoid preparations from PA340 and PA340-678 was also compared (Figure 2B). Twenty-five percent of PA340 nucleoids displayed a dumbbell-shape, whereas 49% of nucleoids from PA340-678 cells were dumbbells. This difference in the prevalence of dumbbells was dependent on MreB, because overexpression of only *mreB* in PA340-678 cells was sufficient to decrease the predominance of dumbbells to wild-type levels (Figure 2B).

mreB Mutant Strains Are Deficient in Topo IV Activity

Upon establishing that a difference in nucleoid size and a corresponding difference in the prevalence of dumbbell-shaped nucleoids between the wild-type and *Δmre* strains were dependent on MreB, we tested whether these differences were because of a deficiency in Topo IV activity. To this end, nucleoids purified from PA340 and PA340-678 were incubated with Topo IV for 2 h and nucleoid size and the incidence of dumbbells were analyzed (Figure 2A). Before Topo IV treatment, 80% of wild-type nucleoids had an area of less than 2 μm^2. After Topo IV treatment for 2 h, 100% of these nucleoids had an area of less than 2 μm^2 in size. Interestingly, after Topo IV treatment, more than 90% of nucleoids from *Δmre* mutants also populated a size class of less than 2 μm^2 in area (Figure 2A). Thus, treatment with Topo IV eliminated the size difference between nucleoids purified from wild-type and *Δmre* strains (mean area 1 μm^2 for wild type vs. 1.1 μm^2 for *Δmre*). Similarly, the frequency of dumbbell-shaped nucleoids from the *Δmre* strain decreased sharply after Topo IV treatment and was similar to the frequency of dumbbells from wild-type cells that were treated with Topo IV (Figure 2B).

To verify whether the effect of Topo IV treatment on nucleoids from the *Δmre* strain could be recapitulated *in vivo*, PA340-678 cells were transformed with an inducible vector carrying both *parC* and *parE* (plex*parEC*), Topo IV expression was induced with 50 μM IPTG, and nucleoids were purified and characterized as before. Overexpression of Topo IV resulted in an almost complete restoration of nucleoid size distribution to wild-type levels (Figure 2C). Furthermore, a 50% reduction in the incidence of dumbbell-shaped nucleoids was also observed (with empty vector (plex5B), 30%; with plex*parEC*, 16%). These results suggest that cells lacking MreB have a chromosome segregation defect that can be attributed to a deficiency in Topo IV activity.

We returned to the observation of Kruse et al. (2003) described above that originally suggested to us that Δ*mreB* strains were deficient in Topo IV activity. We asked whether nucleoids prepared from strains where the dominant-negative *mreBD165V* allele was overexpressed could be decatenated by Topo IV (Figure 2D–F). Nucleoids were isolated from PA340 (pTK509) after induction for 2 h of the *lac* promoter-controlled *mreBD165V* gene carried on the pTK509 plasmid. The preparation of nucleoids after overexpression of the dominant-negative *mreB* allele consisted of singlets (33.6%), doublets (23.4%), and mostly very large, distended nucleoid masses (43%) (Figure 2D). These large nucleoid masses are conglomerates, likely made up of chains of non-segregated chromosomes, and are consistent in appearance with the huge nucleoids elaborated *in vivo* (Kruse et al., 2003). The population of conglomerate nucleoids was reduced significantly after Topo IV treatment (23.4%) (Figure 2E). The population of doublets remained roughly the same (22.1%); however, this is because the doublets are intermediates in complete unlinking of the conglomerates to singlets. Note that the population of singlets (54.5%) rises in proportion to the reduction in conglomerates. The effect of Topo IV treatment is clearly evident by the overall reduction in the area of the nucleoids (Figure 2F). The dominant-negative effect of the *mreBD165V* allele also includes interference with MreB helix formation, causing disruption of the helix throughout the cell, with many regions of the filamented cell lacking any obvious MreB helix. These results suggested that Topo IV activity might be modulated by the oligomeric state of MreB. This proved to be the case.

MreB Interacts Functionally with Topo IV

The observation that *mreB* mutants were deficient in Topo IV activity suggested that MreB might function in the timely activation of Topo IV. This possibility was addressed by testing for a functional biochemical interaction between MreB and Topo IV. To this end, MreB was purified to homogeneity and its effect on the unlinking activity of Topo IV was tested using kinetoplast DNA (kDNA) as the substrate. kDNA is mitochondrial DNA obtained from

trypanosomes such as *Crithidia fasciculata* and consists of large networks (~5000) of mostly covalently closed, catenated minicircles (Chen et al., 1995). Because of their high molecular weight, these networks are unable to enter agarose gels. However, type II topoisomerases such as Topo IV and DNA gyrase can unlink the minicircles that can then be detected by agarose gel electrophoresis (Miller et al., 1981).

The effect of increasing concentrations of MreB on kDNA decatenation at a fixed concentration of either Topo IV or DNA gyrase was measured (Figure 3). With increasing MreB concentration, the amount of minicircles entering the gel in each lane decreased correspondingly, indicating that MreB inhibits the decatenation activity of Topo IV (Figures 3A and 3C). In contrast to the effect on Topo IV, MreB had no effect on kDNA unlinking by DNA gyrase (Figures 3B and 3C), the other type II topoisomerase in *E. coli*, suggesting that MreB inhibits Topo IV activity specifically.

MreB is an actin homologue that can be visualized as helical filaments *in vivo* and polymerizes into actin-like filaments *in vitro* (van den Ent et al., 2001). In order to determine which oligomeric form of MreB, monomer or polymer, caused the observed inhibition of Topo IV, polymerization of MreB under kDNA unlinking conditions was assessed by electron microscopy and dynamic light scattering (Figure 4). MreB polymerization at 37 °C as a function of monomer concentration was assessed using dynamic light scattering. There was little difference in the results between incubation for 30 min or overnight. Polymerization could be detected at 6 nM MreB (Figure 4A), indicating that the critical concentration was quite low. Nucleation was slow, as exemplified by the time course of polymerization at 200 nM MreB (Figure 4B). Single filaments of MreB could be observed by electron microscopy after polymerization of 100 nM protein for 30 min at 37 °C (Figures 4D and 4E). These polymerized filaments averaged 190 ± 160 nm in length (Figure 4I). At 1 μM MreB, 30 min of incubation under these conditions yielded polymerized filaments with an average length of 230 ± 80 nm that were considerably thicker than the single filaments observed at 100 nM MreB, indicating some bundling (Figures 4F, 4G, and 4I). However, after 5 min of incubation of 1 μM MreB under the kDNA decatenation reaction conditions there was no polymerization observed (Figure 4C), consistent with the slow nucleation step suggested by the time course (Figure 4B). Incubation at 4 μM concentration yielded even longer filaments (average length 360 ± 100 nm) that were clearly bundled (Figures 4H and 4I). These data clearly indicate that after 5 min of incubation *E. coli* MreB was largely monomeric. In contrast, by 30 min of incubation MreB was polymerized extensively. Because 5 min of incubation corresponds to the reaction time used for the kDNA decatenation assay (Figure 3 and Experimental Procedures), the data from electron microscopy suggest that monomeric MreB causes the observed inhibition of the Topo IV decatenation activity.

The Functional Interaction between Topo IV and MreB Depends on the Oligomeric State of MreB

Because incubation under kDNA decatenation conditions for 30 min effected a change in the oligomeric state of MreB from monomer to a polymer, we asked whether this change also affected the ability of MreB to inhibit kDNA unlinking by Topo IV. To test this, MreB was incubated under kDNA decatenation conditions for 30 min to allow polymerization and the effect of polymerized MreB on Topo IV-catalyzed kDNA decatenation was then compared to that of monomeric MreB (Figure 5). Increasing concentrations of monomeric MreB inhibited kDNA unlinking by Topo IV as observed before; however, polymerized MreB had just the opposite effect on the decatenation activity of Topo IV. In the absence of pre-incubation, 100 nM MreB completely inhibited Topo IV activity. In contrast, pre-incubation of 100 nM MreB stimulated Topo IV activity by three-fold (Figure 5B). These results indicate that the nature of the functional interaction between MreB and Topo IV is dependent on the oligomeric state of

MreB; monomeric MreB inhibits Topo IV unlinking activity, whereas polymerized MreB stimulates it. In this way, MreB might function as a switch to regulate Topo IV activity.

MreB Interacts Physically with ParC

Having established that MreB interacts functionally with Topo IV, we assessed whether this functional interaction correlated with a physical interaction between MreB and Topo IV components. To this end, purified HA-tagged ParC was incubated with a fraction of polymerized MreB at 37 °C for 1 h and the mixture was then incubated with anti-HA-conjugated agarose beads. After binding for 2.5 hours at 4 °C, the beads were washed and analyzed by SDS-PAGE. In contrast to anti HA-agarose beads alone, HA-ParC conjugated agarose beads were able to retain MreB (Figure 6A), suggesting that MreB physically interacts with ParC. The amount of MreB bound was nearly equal to the amount of ParE bound by HA-ParC (Figure 6A). These results suggest that filamentous MreB physically interacts with Topo IV (as does monomeric MreB, data not shown) and that this physical interaction is likely mediated by the ParC subunit of Topo IV.

To test the specificity of the physical interaction between ParC and MreB, the analogous component of gyrase, GyrA, was conjugated similarly to anti HA-agarose and the ability of MreB to bind HA-GyrA was investigated (Figure 6B). In contrast to HA-ParC, HA-GyrA was unable to bind MreB. Taken together, these results suggest that the specificity of the functional interaction between MreB and Topo IV extends to a physical interaction between the two proteins and indicates that this physical interaction may be important for the ability of MreB to regulate Topo IV activity.

DISCUSSION

Three events dominate the cell cycle in all organisms: DNA replication, chromosome segregation, and cell division. In eukaryotic cells, these events are temporally separated and the oscillating activity of cyclin-dependent kinases together with checkpoint controls ensure that these events are properly ordered with respect to each other (Lew DJ, 1997). In rapidly growing bacteria, DNA replication, chromosome segregation, and cell division overlap significantly. Despite this, these events must be synchronized such that one event is completed prior to the completion of the next event. In an attempt to understand how the completion of chromosome segregation is regulated in *E. coli*, this study has revealed a functional interaction between Topo IV and the cytoskeletal protein MreB. This interaction could explain how late cell cycle events are coordinated to ensure proper chromosome segregation in this organism (Figure 7).

mreB Mutant Strains Have Defects in Chromosome Decatenation

In a previous study (Kruse et al., 2003), analysis by flow cytometry showed that chromosomes segregate in pairs in *ΔmreB* mutants. Furthermore, overexpression of *mreB* alleles carrying mutations in the conserved ATP-binding domain displayed dominant-negative effects, disrupting MreB filaments and blocking chromosome segregation and cell division (Kruse et al., 2003). The authors proposed that MreB filaments actively moved the chromosomes in opposite directions and that the phenotypes of *mreB* mutants are caused by the inability of these mutants to move their chromosomes apart (Kruse et al., 2003). However, subsequent studies have suggested that MreB does not function as a bacterial mitotic apparatus.

To determine the role of MreB in chromosome segregation, a small molecule, S-(3, 4-dichlorobenzyl)isothiourea (A22), was used to rapidly disassemble MreB filaments in *C. crescentus* (Gitai et al., 2005). Disruption of MreB filaments blocked segregation of newly replicated origins, but had no effect on bulk chromosome movement (Gitai et al., 2005). Similar

experiments extended these findings to *E. coli* (Kruse et al., 2006). These results led to the proposal that MreB functions in the active transport of only the origin regions; the remainder of the replicated chromosomes were segregated in an MreB-independent manner (Gitai et al., 2005). However, even these observations have been challenged by a recent study showing that transport of origin regions was not affected by disruption of MreB filaments by A22 treatment in *E. coli* (Karczmarek et al., 2007). These results have rendered the role of MreB in chromosome segregation confusing.

Separate from a role for MreB in either the active transport of chromosomal regions or as a force-generating mitotic apparatus, the results with purified nucleoids reported here suggest that the segregation defects in Δ*mreB* strains are caused by a failure to activate Topo IV in a timely manner. Analysis of compact nucleoids from wild-type and *Δmre* cells indicates that the chromosome segregation defect observed by flow-cytometry in *ΔmreB* strains (Kruse et al., 2003) manifests as a difference in nucleoid size and in the prevalence of dumbbell-shaped nucleoids. This segregation defect in *Δmre* strains can be resolved by treatment of purified nucleoids from *Δmre* cells with Topo IV *in vitro* or suppressed by overexpression of Topo IV in *Δmre* strains *in vivo*. It is possible that the suppression by Topo IV could result from an indirect effect of Topo IV on the topology of the nucleoid. In addition to being a potent decatenase, Topo IV can also relax both negatively and positively supercoiled DNA *in vitro* (Stone et al., 2003) and *in vivo* (Zechiedrich et al., 2000). However, DNA relaxation by Topo IV is unlikely to cause a reduction in nucleoid size. On the other hand, the ability of polymerized MreB to stimulate Topo IV activity *in vitro*, the similar phenotypes of cells carrying dominant-negative alleles of MreB and Topo IV, and the ability of Topo IV to resolve catenated nucleoids from cells overexpressing dominant-negative alleles of *mreB*, suggest that *mreB* mutants have a defect in the timely decatenation of replicated daughter chromosomes.

MreB Confers Timely Oscillation of Topo IV Activity

The unlinking of replicated chromosomes by Topo IV is a terminal event in chromosome segregation (Sherratt et al., 2001). Several lines of evidence, including the localization patterns of Topo IV subunits (Espeli et al., 2003a; Wang and Shapiro, 2004), the demonstration of a Topo IV DNA cleavage hotspot at *dif* (Hojgaard et al., 1999), and the observation by TUNEL (terminal deoxynucleotidyl transferase mediated dUTP nick end labeling) staining of Topo IV-mediated DSBs at septum-proximal edges of nucleoids (Espeli et al., 2003a), suggest that this unlinking occurs at mid-cell. In addition, Topo IV activity is tightly regulated such that active Topo IV is assembled only late in the cell cycle, after DNA replication is completed, when ParC is released from sequestration and can associate with ParE (Espeli et al., 2003a). These results suggest that a mechanism must exist for the timely activation of Topo IV during the cell cycle and for its inactivation soon after the daughter chromosomes are unlinked.

The mechanism by which MreB could confer the observed oscillation in Topo IV activity is described in Figure 7. The observation that *mreB* mutants are deficient in Topo IV activity, together with the ability of polymerized MreB to stimulate the unlinking activity of Topo IV (Figure 5A) suggests that polymerized MreB at mid-cell may function in the activation of Topo IV. This active Topo IV unlinks the replicated chromosomes to complete chromosome segregation. Completion of chromosome segregation clears the way for septum closure to proceed. The bacterial cytoskeleton would require remodeling to facilitate septum closure and completion of cell division. This remodeling entails disassembly of MreB filaments at mid-cell and their reorganization in the daughter cells. The disassembly of MreB filaments produces monomeric MreB, which inhibits Topo IV activity and resets the oscillation of Topo IV activity in the daughter cells.

This model makes two predictions about the regulation of Topo IV activity by MreB. First, in order to differentially regulate Topo IV activity, the oligomeric state of MreB itself must

oscillate between the polymerized and the monomeric forms. Second, this oscillation must spatially and temporally coincide with the spatial and temporal oscillation of Topo IV activity during the bacterial cell cycle. These predictions are supported by several observations. In synchronized stalked cells of *C. crescentus*, MreB was shown to transiently switch from helical structures that extended along the long axis of the cell to a ring-like structure at mid-cell (Figge et al., 2004; Gitai et al., 2004). Moreover, the timing of MreB ring formation coincided with the initiation of cell division and was dependent on the tubulin homologue, FtsZ, which initiates sequential assembly of the division machinery at future division sites (Figge et al., 2004; Gitai et al., 2004). Similarly, in *Rhodobacter sphaeroides*, MreB assembled as a ring at mid-cell at the time of division and disassembled just prior to septation (Slovak et al., 2005).

Recently, the dynamics of MreB during the course of the cell cycle was also characterized in *E. coli* (Vats and Rothfield, 2007). As in other gram-negative bacteria mentioned above, MreB formed a single ring-like structure at mid-cell in an FtsZ-dependent manner. This was followed by reorganization of the single ring into two adjacent rings. Initially, the two rings were linked by an extended helical filament. However, this filament soon disappeared and the two rings gradually moved apart, ultimately extending into new helices in the daughter cells (Vats and Rothfield, 2007). Based on this, it was proposed that the ring-like structures were intermediates of cytoskeletal segregation during the cell cycle (Vats and Rothfield, 2007). These studies support the idea that the MreB cytoskeleton is dynamically remodeled just prior to the onset of cell division, at a time that fits well with the manifestation of Topo IV activity during the cell cycle. Furthermore, this remodeling would cause MreB to oscillate between polymerized and monomeric forms at the cell center, thereby allowing it to differentially regulate Topo IV.

Topo IV Activity Must Be Tightly Regulated During the Cell Cycle

Several studies have reported that Topo IV activity is spatially and temporally regulated during the bacterial cell cycle (Espeli et al., 2003a). On the other hand, a mutation in *dnaX* that causes mis-localization of ParC during the cell cycle also causes extreme filamentation (Espeli et al., 2003a). Furthermore, overproduction of either Topo IV (Espeli et al., 2003b) or ParC alone (Nurse et al., 2003) is toxic to the cell, suggesting that promiscuous Topo IV activity may compromise cell viability. This observation could perhaps explain why overexpression of Topo IV only partially rescues the segregation defects of *Δmre* mutants. Thus, inhibition of Topo IV by monomeric MreB after the completion of chromosome segregation could protect cells from the perils of unrestricted Topo IV activity. If MreB functions in the timely oscillation of Topo IV activity, why don't *ΔmreB* mutants display the deleterious effects of unregulated Topo IV activity? On one hand, it is possible that the deficiency of Topo IV activity in cells lacking MreB compensates for the normally deleterious effects of promiscuous Topo IV activity. Alternatively, several mechanisms may function in the inactivation of Topo IV and some of these mechanisms may be independent of MreB. For example, the replication machinery is known to sequester ParC away from ParE (Espeli et al., 2003a; Wang and Shapiro, 2004).

MreB Facilitates Chromosome Segregation in Multiple Ways

The cytoskeleton mediates important functions in the eukaryotic cell cycle. During mitosis, an elaborate spindle of microtubules orchestrates chromosome segregation and actin forms the cytokinetic ring (Carballido-Lopez and Errington, 2003). The discovery of bacterial homologues of tubulin and actin revealed a role reversal with respect to the cellular localization of these proteins — the tubulin homologue, FtsZ, was found to form the cytokinetic Z ring, whereas actin homologues like MreB formed helical networks that spanned the length of the bacterial cell (Kruse and Gerdes, 2005). Subsequent studies have revealed roles for MreB in the maintenance of cell shape, determination of cell polarity, cell division, and chromosome segregation (Carballido-Lopez, 2006).

In the context of chromosome segregation, previous studies investigated a role for MreB in generating the force for chromosome segregation. These studies revealed that MreB functions in the bipolar transport of origin-proximal regions (Gitai et al., 2005; Kruse et al., 2006). It was also shown that MreB interacts with RNA polymerase and it was proposed that this interaction is functionally significant for chromosome segregation (Kruse et al., 2006). In addition, our study has revealed that MreB functions in chromosome segregation by regulating Topo IV activity. Together, these results suggest that MreB performs multiple functions to ensure proper chromosome segregation. In this regard, MreB shows similarity to the microtubule spindle. In eukaryotic cells, the microtubule spindle is involved in a number of functions including chromosome capture and chromosome congression, besides actively segregating replicated chromosomes (Maiato et al., 2004). Microtubulues also help position and specify the cleavage site during cytokinesis (Maiato et al., 2004).

The observation that MreB can differentially regulate Topo IV depending on its oligomeric state also has precedents in actin. In eukaryotes, many actin binding proteins such as thymosin β4 interact strongly with monomeric G-actin but not with polymerized F-actin. F-actin and G-actin have also been shown to interact differentially with DNase I (Cooper and Pollard, 1982). Monomeric G-actin binds tightly to DNase I in a 1:1 complex and inhibits the hydrolytic activity of DNase I. In contrast, DNase I binds only weakly to F-actin and slowly causes depolymerization of F-actin. This study has shown that MreB specifically interacts with the ParC subunit of Topo IV. However, it is not known whether Topo IV interacts with equal affinity to monomeric and polymerized MreB, nor do we know the mechanism by which MreB stimulates Topo IV activity. Answering these questions about the mechanism by which MreB regulates Topo IV activity, as well as mapping the details of the MreB-Topo IV physical interaction, should further illuminate the functions mediated by the bacterial cytoskeleton in orchestrating chromosome segregation.

EXPERIMENTAL PROCEDURES

E.coli Strains, Plasmids, and Isolation of Compact Nucleoids

PA340 (wild type) and PA340-678 (*Δmre*) were gifts of M. Wachi (Tokyo Institute of Technology, Yokohama, Japan). Plasmid pTK509 was the gift of Kenn Gerdes (University of Southern Denmark). C600 and C600*parC1215* were as described (Espeli et al., 2003b). plex*parEC* carries both *parC* and *parE* under the control of an IPTG-inducible promoter in a modified plex5BA plasmid as described previously (Mossessova et al., 2000). For purification of nucleoids, cells were grown in LB media at 37 °C to an OD_{600} of 0.25, DAPI was added to a concentration of 0.5 μg/ml, and cells were allowed to grow to an OD_{600} of 0.4. For C600 and C600*parC1215*, cells were grown at 30 °C and then shifted to 37 °C for 40 min. Nucleoids were isolated in their compact form as described previously (Zimmerman and Murphy, 2001). Aliquots (5 μl) were mixed with an equal volume of 2% low melting agarose (in 20 mM sodium diethylmalonate [pH 7.1]), the nucleoids were spread on slides, and visualized by fluorescent microscopy (Olympus AX70, 40X magnification). Nucleoid size was measured using the integrated morphometry analysis tool of Metamorph software (version 6.3, Universal Imaging).

Nucleoid Decatenation Assay

Decatenation of compact nucleoids was carried out as described (Espeli et al., 2003a). Reaction mixtures (100 μl final) containing 50 mM Tris-HCl (pH 8.0 at 4 °C), 6 mM $MgCl_2$, 20 mM KCl, 10 mM DTT, 1 mM ATP, 3 μl purified nucleoids (as prepared above), and 2 μM Topo IV were incubated at 37 °C for 2 h. The reactions were stopped using 20 mM EDTA and nucleoids were visualized and characterized as described above.

Purification of MreB

BL21(λDE3)plysS(pET11c-*mreB*) was grown at 37 °C in 12 L of LB broth to an OD_{600} of 0.4 and induced with 0.4 mM IPTG for 2 h. Cells were harvested by centrifugation, resuspended in 15 ml 10 mM Tris-HCl (pH 8.0 at 4 °C), 10% sucrose, and frozen at −80 °C. Cells were thawed and mixed with 50 ml lysis buffer (50 mM Tris-HCl [pH 8.0 at 4°C], 50 mM KCl, 5 mM DTT, 0.3 mM $MgCl_2$, 0.3 mM ATP, 1% Triton X-100, 10% sucrose) for 10 min at 0 °C, and then centrifuged at 100,000 × g for 75 min at 4 °C. MreB was precipitated from the supernatant by adding solid $(NH_4)_2SO_4$ to 45% saturation. The precipitate was resuspended in 15 ml buffer A (50 mM Tris-HCl [pH 8.0 at 4 °C], 50 mM KCl, 5 mM DTT, 0.3 mM $MgCl_2$, 0.3 mM ATP, 0.1% Triton X-100, 20% glycerol), re-precipitated by adding solid $(NH_4)_2SO_4$ to 35% saturation, and the precipitate resuspended in 10 ml buffer A (fraction 1; 117 mg protein). Fraction 1 was loaded onto an ATP-saturated Q-Sepahrose column (34 ml; Amersham). The column was washed with 100 ml buffer A and MreB was eluted with a linear gradient (340 ml) of 150–500 mM KCl in buffer A. MreB eluted at 260 mM KCl (fraction 2; 34 mg protein). Fraction 2 was loaded onto an ATP-saturated DEAE-Sepharose column (20 ml; Amersham). The column was washed with 60 ml buffer A and MreB was eluted with a linear gradient (200 ml) of 100–450 mM KCl in buffer A. MreB eluted at 270 mM KCl (fraction 3; 16 mg protein). Fraction 3 was dialyzed overnight against buffer H (50 mM HEPES-KOH [pH 7.0], 200 mM KCl, 5 mM DTT, 0.3 mM $MgCl_2$, 0.3 mM ATP, 0.1% Triton X-100, 20% glycerol) and loaded onto a 10 ml Biorex 70 (Bio-Rad) column. The column was washed with 30 ml buffer H containing 50 mM KCl and MreB was eluted with a linear gradient (100 ml) of 100–500 mM KCl in buffer H. MreB eluted at 300 mM KCl (fraction 4; 1.5 mg). Purified MreB was concentrated using an Amicon-15 filter by centrifugation for 3 h, dialyzed against storage buffer (50 mM Tris-HCl [pH 8.0 at 4 °C], 100 mM KCl, 5 mM DTT, 0.2 mM ATP, 40% glycerol), aliquoted, and stored at −80 °C.

Decatenation of kDNA

kDNA (TopoGen) decatenation reaction mixtures (10 μl) were prepared as described previously (Nurse et al., 2000). Reaction mixtures were incubated with 0.5 nM Topo IV or 30 nM gyrase and varying amounts of MreB for 4 min at 37 °C. EDTA was then added to a final concentration of 50 mM and the incubation was continued for 2 min. SDS and proteinase K were then added to final concentrations of 1% and 50 μg/ml respectively, and the incubation was continued for an additional 20 min. The reaction products were electrophoresed through 1.4% agarose (SeaKem ME) gels at 2 V/cm for 16 h at room temperature using 50 mM Tris-HCl [pH 7.8 at 23 °C], 40 mM NaOAc, and 1 mM EDTA as the electrophoresis buffer. Gels were stained with SYBR Gold (Invitrogen) for 30 min, images were recorded using a Fuji FLA 5000 laser scanning fluorimeter, and the amount of DNA products was quantified using ImageGuage software (Fuji). In reactions that used polymerized MreB, the kDNA reaction mix was pre-incubated with the appropriate amount of MreB at 37 °C for 30 min prior to the addition of Topo IV.

MreB Polymerization

To measure polymerization of MreB by dynamic light scattering, protein at the indicated concentrations was incubated in a buffer containing 50 mM Tris [pH 8.0 at 4°C], 6 mM MgOAc, 10 mM DTT, 1 mM ATP, and 100 mM potassium glutamate at 37°C. Light scattering intensity was measured at 90° from the axis of incident light using a Dyna Pro (Wyatt instruments, Santa Barbara, CA) system. Measurements were analyzed using Dynamics software (Protein solutions, inc.). The critical concentration determination and kinetics of MreB polymerization were performed essentially as described in Bean and Amann (2008). To determine the critical concentration, MreB at various concentrations was incubated with the kDNA reaction buffer at 37 °C for either 30 min or overnight. Light scattering counts were

averaged over 1 min of the acquired signal as described above. For determination of the kinetics of MreB polymerization, MreB was diluted to 200 nM in kDNA reaction buffer on ice, incubated at 37 °C for the indicated times, and light scattering counts were measured as described above. For electron microscopy, MreB was diluted to the indicated concentrations in kDNA reaction buffer and incubated for either 5 min or 30 min at 37 °C. Samples were prepared for electron microscopy as described by Esue et al. (2005). Images were acquired using a Jeol 1200 EX transmission electron microscope (120,000 X magnification) and were analyzed using the measurement tool of AMT software (AMT Corp.)

Binding of MreB to HA-ParC and HA-Gyrase

Monoclonal anti-HA conjugated agarose beads (Sigma) were washed twice with 0.1 M glycine (pH 2.5), and resuspended in binding buffer (50 mM Tris-HCl [pH 8.0 at 4 °C], 5 mM $MgCl_2$, 1 mM EDTA, 100 mM NaCl, 0.05% NP-40, 10% glycerol). For the binding reactions (100 μl), either HA-ParC or HA-GyrA (0.2 μM final concentration) was mixed with an eight-fold molar excess of the indicated proteins and incubated at 37 °C for 1 h. Following this, the protein mixtures were incubated with 10 μl of anti-HA conjugated agarose beads for 2.5 h at 4 °C. The beads were then pelleted, washed twice with 100 μl binding buffer, boiled in Laemmli SDS-PAGE loading dye, and analyzed by 8% SDS-PAGE.

Acknowledgments

We thank Dr. Hao Wu, Pearl Nurse, and the SKI EM facility for technical assistance. These studies were supported by NIH grant GM 34558.

References

Adams DE, Shekhtman EM, Zechiedrich EL, Schmid MB, Cozzarelli NR. The role of topoisomerase IV in partitioning bacterial replicons and the structure of catenated intermediates in DNA replication. Cell 1992;71:277–288. [PubMed: 1330320]

Bean GJ, Amann KJ. Polymerization properties of the *Thermotoga maritima* actin MreB: roles of temperature, nucleotides, and ions. Biochemistry 2008;47:826–835. [PubMed: 18095710]

Carballido-Lopez R. The bacterial actin-like cytoskeleton. Microbiol Mol Biol Rev 2006;70:888–909. [PubMed: 17158703]

Carballido-Lopez R, Errington J. A dynamic bacterial cytoskeleton. Trends Cell Biol 2003;13:577–583. [PubMed: 14573351]

Chen J, Rauch CA, White JH, Englund PT, Cozzarelli NR. The topology of the kinetoplast DNA network. Cell 1995;80:61–69. [PubMed: 7813018]

Cooper JA, Pollard TD. Methods to measure actin polymerization. Methods Enzymol 1982;85:182–210. [PubMed: 6889668]

Espeli O, Levine C, Hassing H, Marians KJ. Temporal regulation of topoisomerase IV activity in E. coli. Mol Cell 2003a;11:189–201. [PubMed: 12535532]

Espeli O, Marians KJ. Untangling intracellular DNA topology. Mol Microbiol 2004;52:925–931. [PubMed: 15130115]

Espeli O, Nurse P, Levine C, Lee C, Marians KJ. SetB: an integral membrane protein that affects chromosome segregation in *Escherichia coli*. Mol Microbiol 2003b;50:495–509. [PubMed: 14617174]

Esue O, Cordero M, Wirtz D, Tseng Y. The assembly of MreB, a prokaryotic homolog of actin. J Biol Chem 2005;280:2628–2635. [PubMed: 15548516]

Figge RM, Divakaruni AV, Gober JW. MreB, the cell shape-determining bacterial actin homologue, co-ordinates cell wall morphogenesis in *Caulobacter crescentus*. Mol Microbiol 2004;51:1321–1332. [PubMed: 14982627]

Gitai Z, Dye N, Shapiro L. An actin-like gene can determine cell polarity in bacteria. Proc Nat'l Acad Sci USA 2004;101:8643–8648.

Gitai Z, Dye NA, Reisenauer A, Wachi M, Shapiro L. MreB actin-mediated segregation of a specific region of a bacterial chromosome. Cell 2005;120:329–341. [PubMed: 15707892]

Hojgaard A, Szerlong H, Tabor C, Kuempel P. Norfloxacin-induced DNA cleavage occurs at the dif resolvase locus in *Escherichia coli* and is the result of interaction with topoisomerase IV. Mol Microbiol 1999;33:1027–1036. [PubMed: 10476036]

Karczmarek A, Martinez-Arteaga R, Alexeeva S, Hansen FG, Vicente M, Nanninga N, den Blaauwen T. DNA and origin region segregation are not affected by the transition from rod to sphere after inhibition of *Escherichia coli* MreB by A22. Mol Microbiol 2007;65:51–63. [PubMed: 17581120]

Kato J, Nishimura Y, Imamura R, Niki H, Hiraga S, Suzuki H. New topoisomerase essential for chromosome segregation in *E. coli*. Cell 1990;63:393–404. [PubMed: 2170028]

Kato J, Nishimura Y, Yamada M, Suzuki H, Hirota Y. Gene organization in the region containing a new gene involved in chromosome partition in *Escherichia coli*. J Bacteriol 1988;170:3967–3977. [PubMed: 2842295]

Kruse T, Blagoev B, Lobner-Olesen A, Wachi M, Sasaki K, Iwai N, Mann M, Gerdes K. Actin homolog MreB and RNA polymerase interact and are both required for chromosome segregation in *Escherichia coli*. Genes Dev 2006;20:113–124. [PubMed: 16391237]

Kruse T, Bork-Jensen J, Gerdes K. The morphogenetic MreBCD proteins of *Escherichia coli* form an essential membrane-bound complex. Mol Microbiol 2005;55:78–89. [PubMed: 15612918]

Kruse T, Gerdes K. Bacterial DNA segregation by the actin-like MreB protein. Trends Cell Biol 2005;15:343–345. [PubMed: 15922599]

Kruse T, Moller-Jensen J, Lobner-Olesen A, Gerdes K. Dysfunctional MreB inhibits chromosome segregation in *Escherichia coli*. The EMBO J 2003;22:5283–5292.

Lew, DJWT.; Pringle, JR. Cell Cycle Control in Saacharomyces cerevisiae. In: Pringle, JR.; Jones, EW., editors. The Molecular and Cellular Biology of the Yeast Saacharomyces. Plainview, New York: Cold Spring Harbor Laboratory Press; 1997. p. 607-695.

Maiato H, Sampaio P, Sunkel CE. Microtubule-associated proteins and their essential roles during mitosis. International Rev Cytol 2004;241:53–153.

Miller KG, Liu LF, Englund PT. A homogeneous type II DNA topoisomerase from HeLa cell nuclei. J Biol Chem 1981;256:9334–9339. [PubMed: 6267071]

Mohammadi T, Karczmarek A, Crouvoisier M, Bouhss A, Mengin-Lecreulx D, den Blaauwen T. The essential peptidoglycan glycosyltransferase MurG forms a complex with proteins involved in lateral envelope growth as well as with proteins involved in cell division in *Escherichia coli*. Mol Microbiol 2007;65:1106–1121. [PubMed: 17640276]

Mossessova E, Levine C, Peng H, Nurse P, Bahng S, Marians KJ. Mutational analysis of *Escherichia coli* topoisomerase IV. I Selection of dominant-negative *parE* alleles. J Biol Chem 2000;275:4099–4103. [PubMed: 10660569]

Nurse P, Bahng S, Mossessova E, Marians KJ. Mutational analysis of *Escherichia coli* topoisomerase IV. II ATPase negative mutants of *parE* induce hyper-DNA cleavage. J Biol Chem 2000;275:4104–4111. [PubMed: 10660570]

Nurse P, Levine C, Hassing H, Marians KJ. Topoisomerase III can serve as the cellular decatenase in *Escherichia coli*. J Biol Chem 2003;278:8653–8660. [PubMed: 12509418]

Peng H, Marians KJ. Decatenation activity of topoisomerase IV during *oriC* and pBR322 DNA replication in vitro. Proc Nat'l Acad Sci USA 1993;90:8571–8575.

Sawitzke JA, Austin S. Suppression of chromosome segregation defects of *Escherichia coli muk* mutants by mutations in topoisomerase I. Proc. Nat'l Acad Sci USA 2000;97:1671–1676.

Sherratt DJ, Lau IF, Barre FX. Chromosome segregation. Curr Opin Microbiol 2001;4:653–659. [PubMed: 11731316]

Slovak PM, Wadhams GH, Armitage JP. Localization of MreB in Rhodobacter sphaeroides under conditions causing changes in cell shape and membrane structure. J Bacteriol 2005;187:54–64. [PubMed: 15601688]

Soufo HJ, Graumann PL. Actin-like proteins MreB and Mbl from Bacillus subtilis are required for bipolar positioning of replication origins. Curr Biol 2003;13:1916–1920. [PubMed: 14588250]

Steck TR, Drlica K. Bacterial chromosome segregation: evidence for DNA gyrase involvement in decatenation. Cell 1984;36:1081–1088. [PubMed: 6323018]

Stone MD, Bryant Z, Crisona NJ, Smith SB, Vologodskii A, Bustamante C, Cozzarelli NR. Chirality sensing by *Escherichia coli* topoisomerase IV and the mechanism of type II topoisomerases. Proc Nat'l Acad Sci USA 2003;100:8654–8659.

van den Ent F, Amos LA, Lowe J. Prokaryotic origin of the actin cytoskeleton. Nature 2001;413:39–44. [PubMed: 11544518]

Vats P, Rothfield L. Duplication and segregation of the actin (MreB) cytoskeleton during the prokaryotic cell cycle. Proc Nat'l Acad Sci USA 2007;104:17795–17800.

Wang SC, Shapiro L. The topoisomerase IV ParC subunit colocalizes with the Caulobacter replisome and is required for polar localization of replication origins. Proc Nat'l Acad Sci USA 2004;101:9251–9256.

Zechiedrich EL, Khodursky AB, Bachellier S, Schneider R, Chen D, Lilley DM, Cozzarelli NR. Roles of topoisomerases in maintaining steady-state DNA supercoiling in *Escherichia coli*. J Biol Chem 2000;275:8103–8113. [PubMed: 10713132]

Zimmerman SB, Murphy LD. Release of compact nucleoids with characteristic shapes from *Escherichia coli*. J of Bacteriol 2001;183:5041–5049. [PubMed: 11489856]

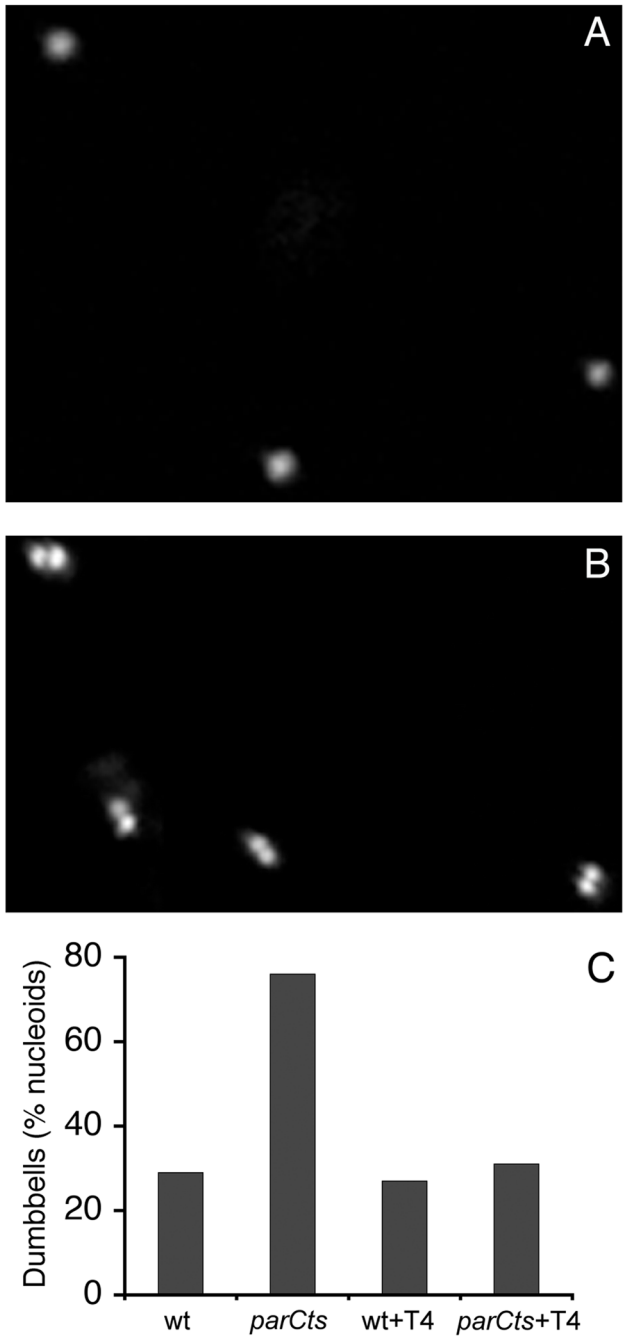

Figure 1. Dumbbell-shaped Nucleoids Are Intermediates of Chromosome Segregation

Compact nucleoids were purified from C600 and C600*parC1215*, visualized by fluorescence microscopy after staining with DAPI, and the prevalence of dumbbells was assessed. Approximately 300 nucleoids were examined for each experiment.

(A) and (B) Two morphologically distinct classes are present in nucleoids purified from *E.coli* cells: (A) Singlets and (B) dumbbells.

(C) Dumbbell-shaped nucleoids are enriched in *parC* mutants and can by resolved by Topo IV *in vitro*.

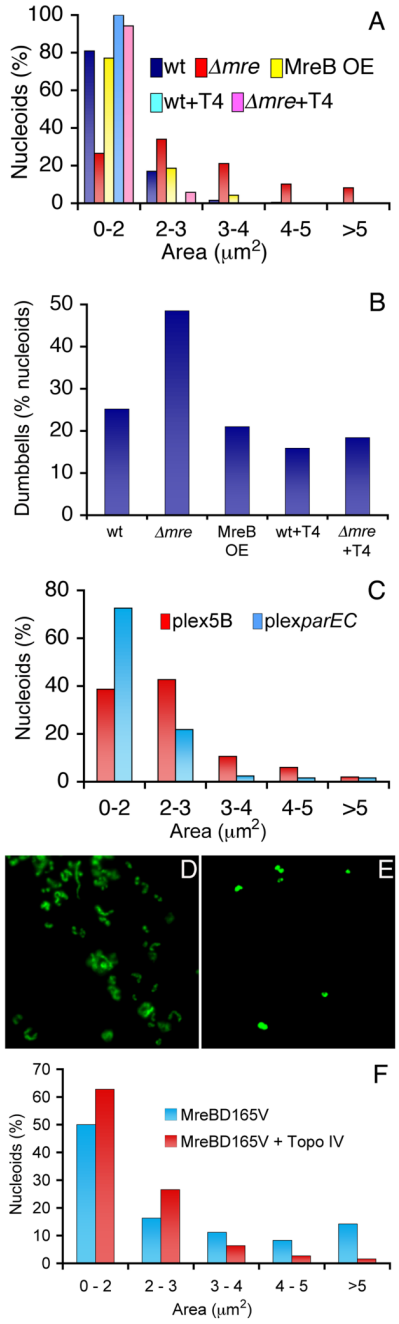

Figure 2. *mreB* Mutant Strains Are Deficient in Topo IV Activity

Compact nucleoids were isolated from the indicated strains, visualized by DAPI staining, their areas were measured, and the prevalence of dumbbells was assessed. Approximately 300 nucleoids were examined for each experiment.

(A) Distribution of nucleoid sizes in preparations from either wild-type (wt) or *Δmre* cells that either had or had not been treated with Topo IV; as well as from wild-type cells where MreB had been overexpressed.

(B) Incidence of dumbbell-shaped nucleoids from (A).

(C) Nucleoid size distribution after Topo IV overexpression in *Δmre* strains.

(D) Nucleoids isolated from PA340(pTK509) after 2 h of induction of the ectopic *mreBD165V* gene.
(E) Nucleoids from (D) after treatment with Topo IV
(F) Size distribution of nucleoids from (D) and (E).

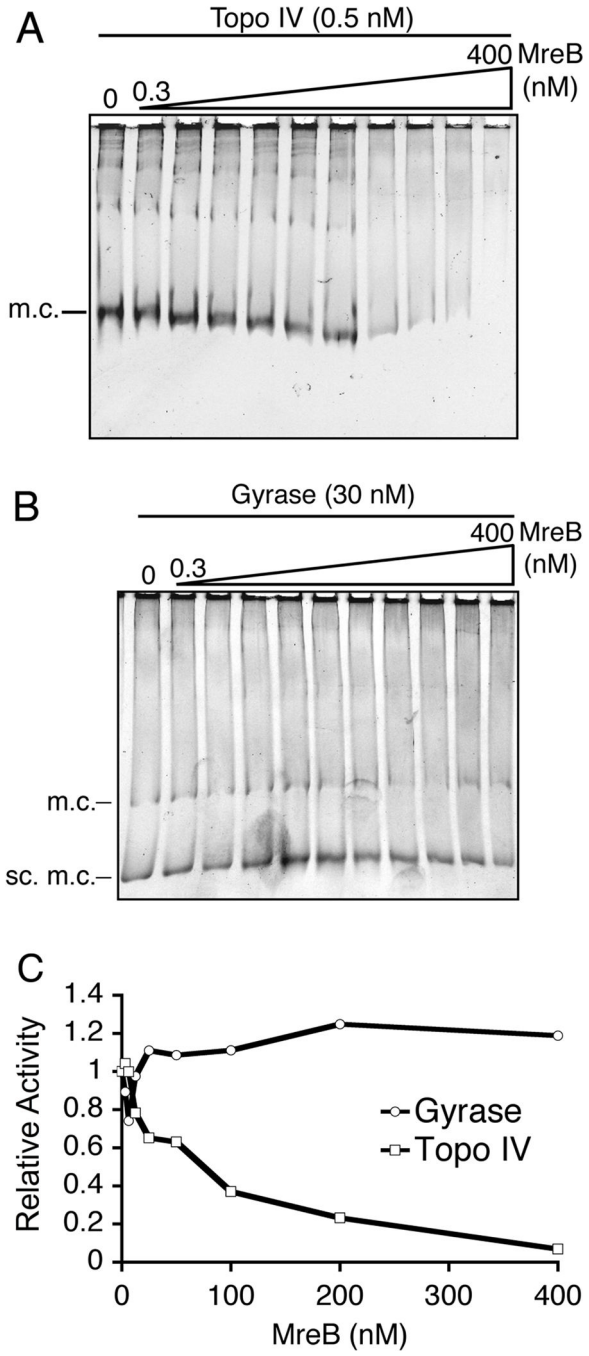

Figure 3. MreB Specifically Inhibits Decatenation of kDNA by Topo IV

kDNA decatenation reaction mixtures were incubated with either 0.5 nM Topo IV or 30 nM gyrase and the indicated amounts of MreB for 4 min at 37 °C. The reaction products were electrophoresed through 1.4% agarose gels, stained with SYBR Gold, and quantified as described under Experimental Procedures. The amount of kDNA minicircles produced by Topo IV or Gyrase in the absence of MreB was assigned a value of 1 and decatenation in the presence of MreB was expressed relative to this number.

(A) and (B) Effect of increasing concentrations of MreB on kDNA decatenation catalyzed by (A) Topo IV and (B) gyrase.

(C) Quantification of data shown in panels (A) and (B). Shown is an average of three measurements each for Topo IV and gyrase. m.c., minicircles; sc. m.c., supercoiled minicircles.

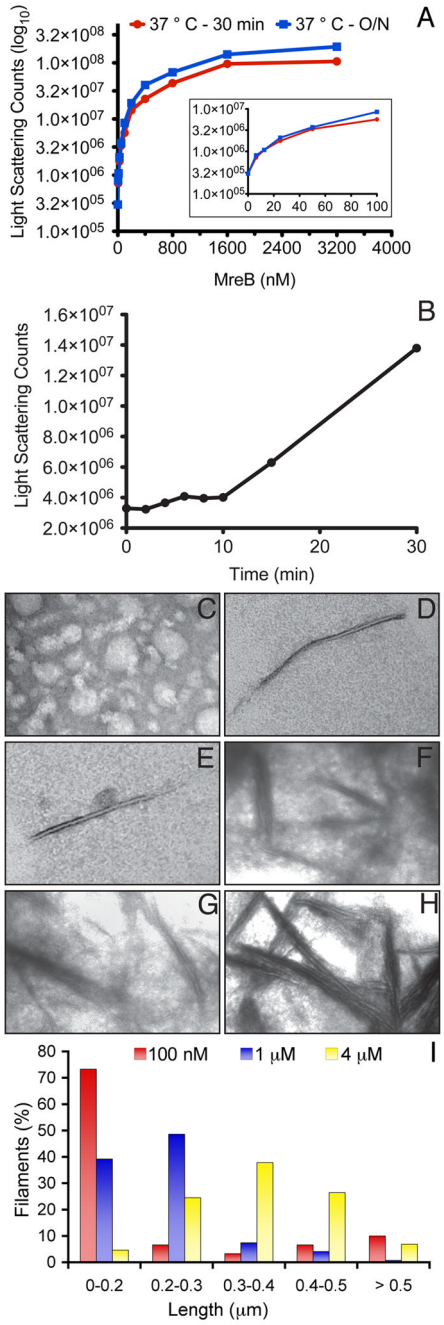

Figure 4. Analysis of MreB Polymerization Under kDNA Decatenation Conditions

(A) MreB polymerization as a function of total monomer concentration. MreB was diluted to the indicated concentrations in kDNA reaction buffer and incubated at 37°C for either 30 min or overnight. Light scattering counts were then measured as described in Experimental Procedures. The inset gives an exploded view of the results for 6.25 nM – 100 nM MreB.

(B) Kinetics of MreB polymerization. MreB was diluted to a concentration of 200 nM in kDNA reaction buffer and incubated at 37 °C for the indicated times. Light scattering counts were then measured as in (A).

(C) – (H) Electron microscopic ananlysis of MreB filaments. MreB was diluted to a concentration of either 100 nM (D and E), 1 μM (C, F, and G), or 4 μM (H) in kDNA reaction

buffer, incubated at 37 °C for either 5 min (C) or 30 min (D–H), and filaments were visualized by electron microscopy as described in Experimental Procedures.
(I) Distribution of filament length at 100 nM, 1 μM, and 4 μM MreB after 30 min of polymerization at 37 °C. About 40 filaments were measured at 100 nM and about 200 filaments were measured at 1 μM and 4 μM MreB respectively.

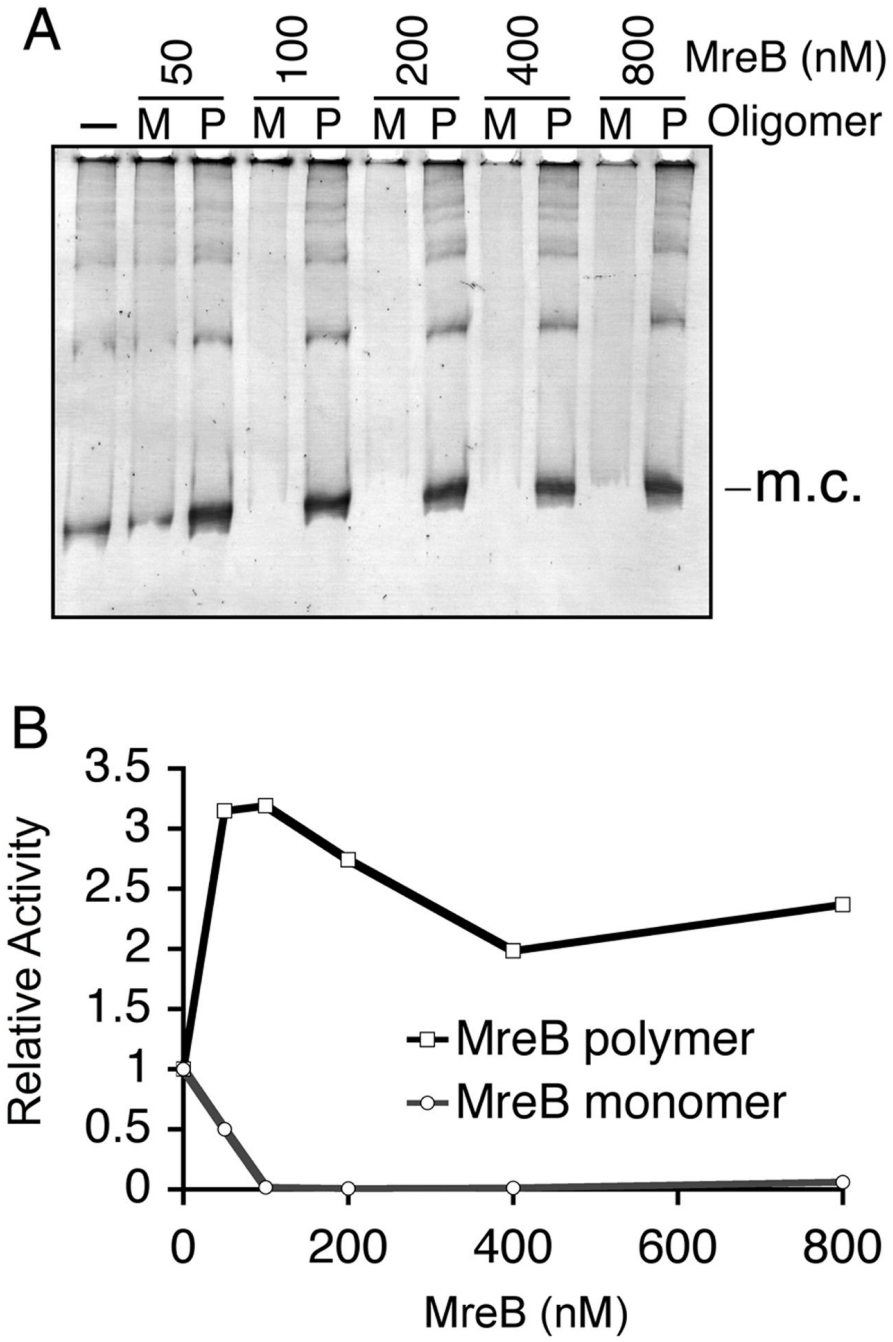

Figure 5. The Oligomeric State of MreB Determines its Effect on Topo IV Decatenation Activity

(A) Two sets of reactions were performed. In one set (lanes marked "M"), MreB was titrated as in Figure 3. In the second set (lanes marked "P"), the indicated amounts of MreB were pre-incubated with the kDNA reaction mix for 30 min at 37 °C prior to the addition of Topo IV. (B) Quantification of (A). Relative activity was measured as in Figure 3.

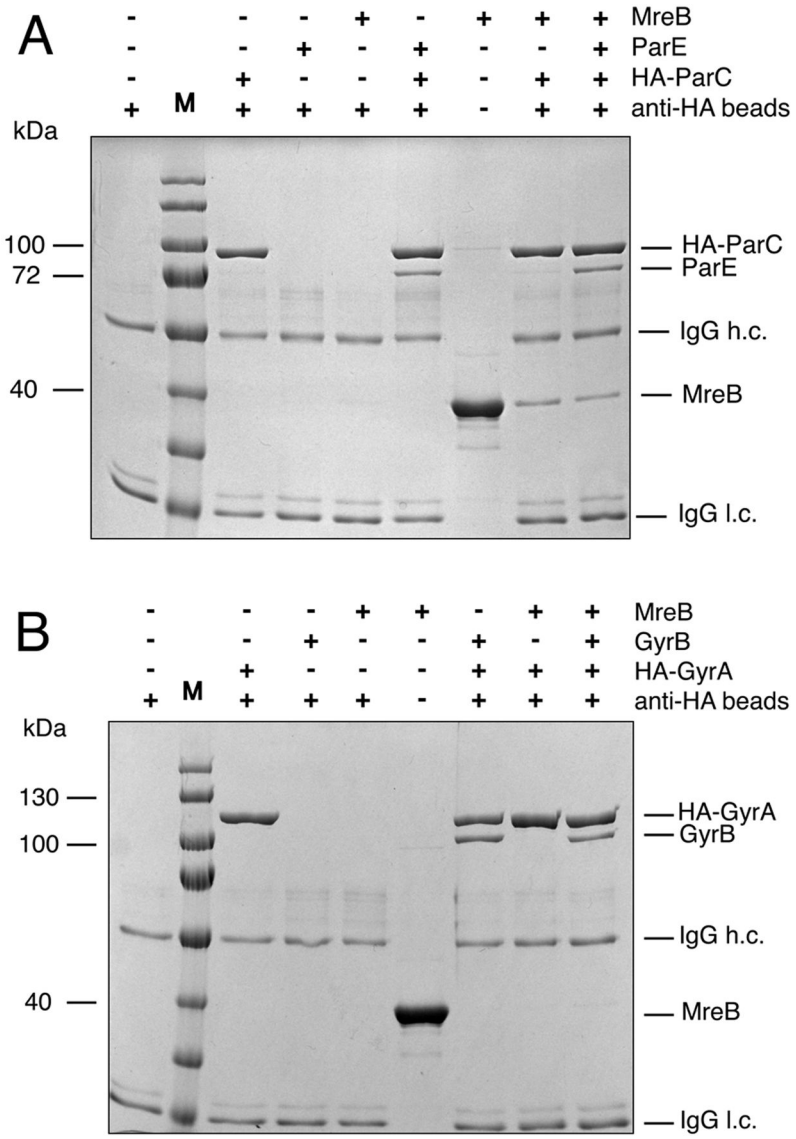

Figure 6. MreB Physically Interacts with ParC

HA-ParC (A) or HA-GyrA (B) was incubated with an eight-fold excess of the indicated proteins and analyzed as described under Experimental Procedures. MreB marker lanes are direct loads of the protein to the gel. h.c., IgG heavy chain; l.c., IgG light chain.

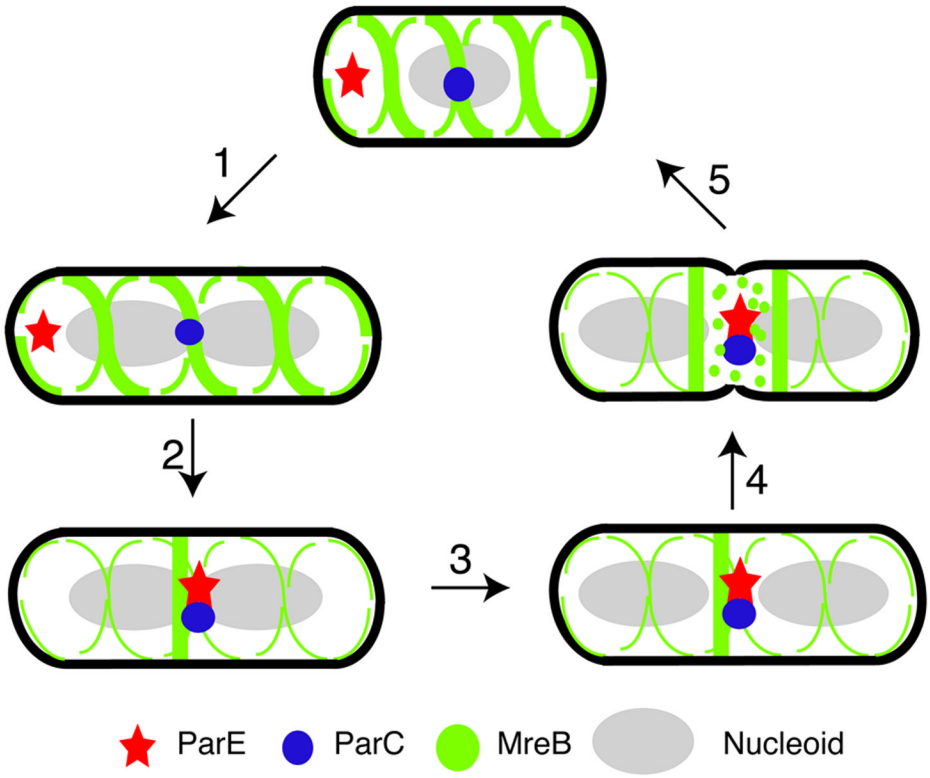

Figure 7. Interaction between MreB and Topo IV May Help Coordinate Late Cell Cycle Events

(1) Topo IV activity is spatially and temporally regulated during the bacterial cell cycle. (2) Active Topo IV is assembled only late in the cell cycle. Meanwhile, remodeling of MreB filaments during the cell cycle causes the accumulation of a ring of polymerized MreB at the cell center. (3) Polymerized MreB stimulates the decatenation activity of Topo IV. (4) MreB filaments are further remodeled to facilitate their segregation to the two daughter cells. This remodeling produces monomeric MreB. (5) Inhibition of Topo IV activity by monomeric MreB restores a state of low Topo IV activity at the onset of a new cell cycle.